

# We are IntechOpen, the world's leading publisher of Open Access books Built by scientists, for scientists

6,900

Open access books available

186,000

International authors and editors

200M

Downloads

Our authors are among the

154

Countries delivered to

TOP 1%

most cited scientists

12.2%

Contributors from top 500 universities



WEB OF SCIENCE™

Selection of our books indexed in the Book Citation Index  
in Web of Science™ Core Collection (BKCI)

Interested in publishing with us?  
Contact [book.department@intechopen.com](mailto:book.department@intechopen.com)

Numbers displayed above are based on latest data collected.  
For more information visit [www.intechopen.com](http://www.intechopen.com)



---

# High Performance PET/Carbon Nanotube Nanocomposites: Preparation, Characterization, Properties and Applications

---

Jun Young Kim and Seong Hun Kim

Additional information is available at the end of the chapter

<http://dx.doi.org/10.5772/50413>

---

## 1. Introduction

Poly(ethylene terephthalate) (PET) is one of aromatic polyesters, widely used polyester resin in conventional industry because of its good mechanical properties, low cost, high transparency, high processability, and moderate recyclability. Thus, PET holds a potential for industrial application, including industrial fibers, films, bottles, and engineering plastics [1–3]. In this regard, much research has been extensively performed to develop commercial application of aromatic polyesters or its composites, such a high performance polymer [4–11]. Although promising, however, insufficient mechanical properties and thermal stability of PET have hindered its practical application in a broad range of industry. From both an economic and industrial perspective, the major challenges for high performance polymer nanocomposites are to fabricate the polymer nanocomposites with low costs and to facilitate large scale-up for commercial applications.

Carbon nanotubes (CNTs), which were discovered by Iijima [12], have attracted a great deal of scientific interest as advanced materials for next generation. The CNT consisting of concentric cylinder of graphite layers is a new form of carbon and can be classified into three types [12–14]: single-walled CNT (SWCNT), double-walled CNT (DWCNT), and multi-walled CNT (MWCNT). SWCNT consists of a single layer of carbon atoms through the thickness of the cylindrical wall with the diameters of 1.0~1.4 nm, two such concentric cylinders forms DWCNT, and MWCNT consists of several layers of coaxial carbon tubes, the diameters of which range from 10 to 50 nm with the length of more than 10  $\mu\text{m}$  [12–14]. The graphite nature of the nanotube lattice results in a fiber with high strength, stiffness, and conductivity, and higher aspect ratio represented by very small diameter and long length

makes it possible for CNTs to be ideal nanoreinforcing fillers in advanced polymer nanocomposites [15]. Both theoretical and experimental approaches suggest the exceptional mechanical properties of CNTs ~100 times higher than the strongest steel at a fraction of the weight [16-19]: The Young's modulus, strength, and toughness of SWCNT shows 0.32~1.47 TPa of Young's modulus, 10~52 GPa of strength, and ~770 J/g of toughness, respectively [18]. For MWCNT, the values of strength, Young's modulus, and toughness were found to be 11-63 GPa, 0.27-0.95 TPa, and ~1240 J/g, respectively [19]. In addition, CNTs exhibit excellent electrical properties and electric current carrying capacity ~1000 times higher than copper wires [20]. In general, MWCNTs show inferior mechanical performance as compared to SWCNTs. However, MWCNTs have a cost advantage, in that they can be produced in much larger quantities at lower cost compared with the SWNT. In addition, MWCNTs are usually individual, longer, and more rigid than SWCNTs. Because of their remarkable physical properties such as high aspect ratio and excellent mechanical strength, MWCNTs are regarded as prospective reinforcing fillers in high performance polymer nanocomposites. For these reasons, extensive research and development have been directed towards the potential applications of CNTs for novel composite materials in a wide range of industrial fields. The fundamental research progressed to date on applications of CNTs also suggests that CNTs can be utilized as promising reinforcements in new kinds of polymer nanocomposites with remarkable physical/chemical characteristics [14].

During the rapid advancement in the materials science and technology, much research has extensively undertaken on high-performance polymer composites for targeted applications in numerous industrial fields. Furthermore, a great number of efforts have been made to develop high-performance polymer nanocomposites with the benefit of nanotechnology [21-25]. Polymer nanocomposites, which is a new class of polymeric materials based on the reinforcement of polymers using nanofillers, have attracted a great deal of interest in fields ranging from basic science to the industrial applications because it is possible to remarkably improve the physical properties of composite materials at lower filler loading [21-25]. These attempts include studies of the polymer composites with the introduction of nanoreinforcing fillers such as CNT, carbon nanofibers, inorganic nanoparticles, and polymer nanoparticles into the polymer matrix [21-25, 35-48]. In particular, excellent mechanical strength, thermal conductivity, and electrical properties of CNT have created a high level of activity in materials research and development for potential applications such as fuel cell, hydrogen storage, field emission display, chemical or biological sensor, and advanced polymer nanocomposites [26-34]. This feature has motivated a number of attempts to fabricate CNT/polymer nanocomposites in the development of high-performance composite materials. In this regard, much research and development have been performed to date for achieving the practical realization of excellent properties of CNT for advanced polymer nanocomposites in a broad range of industrial applications. However, because of their high cost and limited availability, only a few practical applications in industrial field such as electronic and electric appliances have been realized to date. In addition, potential applications as nanofillers have not been fully realized, despite extensive studies on CNT-filled polymer nanocomposites. Therefore, the fabrication of the polymer nanocomposites reinforced with various nanofillers is believed to a key technology on advanced composites for next generation.

For the fabrication of the CNT/polymer nanocomposites, major goal realize the potential applications of CNT as effective nanoreinforcements, leading to high performance polymer nanocomposites, are uniform dispersion of CNT in the polymer matrix and good interfacial adhesion between CNT and polymer matrix [49]. The functionalization of CNT, which can be considered as an effective method to achieve the homogeneous dispersion of CNT in the polymer matrix and its compatibility with a polymer, can lead to the enhancement of interfacial adhesion between CNT and polymer matrix, thereby improving the overall properties of the CNT/polymer nanocomposites [50-53]. Currently, four processing techniques are in common use to fabricate the CNT/polymer nanocomposites in situ polymerization, direct mixing, solution method, and melt compounding. Of these processing techniques, melt compounding has been accepted as the simplest and the most effective method from an industrial perspective because this process makes it possible to fabricate high performance polymer nanocomposites at low process cost, and facilitates commercial scale-up. Furthermore, the combination of a very small quantity of expensive CNT with conventional cheap thermoplastic polymers may provide attractive possibilities for improving the physical properties of polymer nanocomposites using a simple and cost-effective method [35-48].

This chapter focused on the fabrication and characterization of PET/CNT nanocomposites. The PET nanocomposites reinforced with a very small quantity of the modified CNT were prepared by simple melt compounding using a twin-screw extruder to fabricate high-performance polymer nanocomposites at low cost, and the resulting nanocomposites were characterized by means of Fourier transform infrared (FT-IR) spectroscopy, thermogravimetric analysis (TGA), rheological measurement, transmission electron microscopy (TEM), scanning electron microscopy (SEM), tensile testing, and differential scanning calorimetry (DSC) to clarify the effects of modified CNT on the physical properties and non-isothermal crystallization behavior of PET/CNT nanocomposites. This study demonstrates that the mechanical and rheological properties, thermal stability, and the non-isothermal crystallization behavior of PET/CNT nanocomposites were strongly dependent on the dispersion of the modified CNT in the PET matrix and the interfacial interactions between the modified CNT and the PET matrix. This chapter also suggests a simple and cost-effective method that can facilitate the industrial realization of CNT-reinforced PET nanocomposites with enhanced physical properties.

## **2. Fabrication of PET/CNT Nanocomposites**

### **2.1. General features**

PET nanocomposites reinforced with a very small quantity of modified CNT were prepared by melt compounding using a twin-screw extruder to create high performance polymer nanocomposites at low manufacturing cost for practically possible application in a broad range of industry. The introduction of carboxylic acid groups on the surfaces of the nanotube leads to the enhanced interactions between the nanotube and the polymer matrix through hydrogen bonding formation. The thermal stability, mechanical, and rheological

properties of the PET nanocomposites are strongly dependent on the interfacial interactions between the PET and the modified CNT as well as the dispersion of the modified CNT in the PET. The introduction of the nanotube can significantly influence the non-isothermal crystallization behavior of the PET nanocomposites. This study demonstrates that a very small quantity of the modified CNT can substantially improve the thermal stability and mechanical properties of the PET nanocomposites, depending on the dispersion of the modified CNT and the interfacial interactions between the polymer matrix and the modified CNT. The key to improve the overall properties of PET nanocomposites depend on the optimization of the unique geometry and dispersion state of CNT in PET nanocomposites. This study also suggests a simple and cost-effective method that facilitates the industrial realization of PET/CNT nanocomposites with enhanced physical properties.

## 2.2. PET nanocomposites containing modified CNT

Conventional thermoplastic polymer used was the PET with an intrinsic viscosity of 1.07 dl/g, supplied by Hyo Sung Corp., Korea. The nanotubes used are multiwalled CNT (degree of purity > 95%) synthesized by a thermal chemical vapor deposition process, purchased from Iljin Nanotech, Korea. According to the supplier, their length and diameter were 10–30 nm and 10–50  $\mu\text{m}$ , respectively, indicating that their aspect ratio reaches 1000.

The pristine CNT was added to the mixture of concentrated  $\text{HNO}_3$  and  $\text{H}_2\text{SO}_4$  with a volumetric ratio of 1:3 and this mixture was sonicated at 80 °C for 4 h to create the carboxylic acid groups on the nanotube surfaces [50]. After this chemical modification, the carboxylic acid groups-induced CNT (c-CNT) is expected to enhance the chemical affinity of the nanotube with the PET as well as the dispersion of the nanotube in the PET matrix. All materials were dried at 120 °C *in vacuo* for at least 24 h, before use to minimize the effect of moisture. The PET nanocomposites were prepared by a melt compounding in a Haake rheometer (Haake Technik GmbH, Germany) equipped with a twin-screw. The temperature of the heating zone, from the hopper to the die, was set to 270, 280, 285, and 275 °C, and the screw speed was fixed at 20 rpm for the fabrication of the PET nanocomposites, PET was melt blended with the addition of CNT content, specified as 0.1, 0.5, and 1.0 wt% in the polymer matrix, respectively. Upon completion of melt blending, the extruded strands were allowed to cool in the water-bath, and then cut into pellets with constant diameter and length using a rate-controlled PP1 pelletizer (Haake Technik GmbH, Germany)

Chemical structures of CNT and the PET nanocomposites were characterized by means of FT-IR measurement using a Magma-IR 550 spectrometer (Nicolet) in the range of 400–4000  $\text{cm}^{-1}$ . TGA of the PET nanocomposites was performed with a TA Instrument SDF-2960 TGA over a temperature range of 30–800 °C at a heating rate of 10 °C/min under  $\text{N}_2$ . Rheological properties of the PET nanocomposites were performed on an ARES (Advanced Rheometer Expanded System) rheometer (Rheometric Scientific) in oscillation mode with the parallel-plate geometry using the plate diameter of 25 mm and the plate gap setting of 1 mm at 270, 280, and 290 °C, covering the temperature processing windows of the PET nanocomposites. The frequency ranges were varied between 0.05 and 450 rad/s, and the strain amplitude was applied to be within the linear viscoelastic ranges. Morphologies of CNT and the PET nano-

composites were observed using a JEOL 2000FX TEM and a JEOL JSM-6300F SEM. Mechanical properties of the PET nanocomposites were measured with an Instron 4465 testing machine, according to the procedures in the ASTM D 638 standard. The gauge length and crosshead speed were set to 20 mm and 10 mm/min, respectively. Thermal behavior of the PET nanocomposites was measured with a TA Instrument 2010 DSC over a temperature range of 30–295 °C at a scan rate of 10 °C/min under N<sub>2</sub>. Samples were heated to 295 °C at a heating rate of 10 °C/min, held at 295 °C for 10 min to eliminate any previous thermal history and then cooled to room temperature at a cooling rate of 10 °C/min. The non-isothermal crystallization kinetics was investigated by cooling samples from 295 to 30 °C at constant cooling rates of 2.5, 5, 10, 15, and 20 °C/min, respectively. The relative degree of crystallinity,  $X(T)$ , of the PET nanocomposites at various cooling rates can be calculated from the ratio of the area of the exothermic peak up to temperature ( $T$ ) divided by that of the total exotherms of the crystallization

### 3. Influence of Modified CNT on PET Nanocomposites

#### 3.1. CNT modification

The FT-IR spectra of CNT and the PET nanocomposites are shown in Figure 1. The characteristic peaks observed at ~1580 cm<sup>-1</sup> was attributed to the IR-phonon mode of multi-walled CNT [54]. The characteristic peaks observed at 1080, 1190, and 1720 cm<sup>-1</sup>, respectively, for the c-CNT were attributed to the stretching vibrations of the carboxylic acid groups [55]. This result demonstrates that carboxylic acid groups on the surface of the c-CNT were effectively induced via chemical modification. After chemical modification, the c-CNT exhibits less entangled structures as compared to pristine CNT showing some agglomerated structures, indicating that the dispersion of the c-CNT in the PET matrix will be more effective than that of pristine CNT. Thus, it is expected that the functional groups effectively induced on the surface of the nanotube via chemical modification are helpful for enhancing the interactions between the polymer matrix and the nanotube.

As shown in Figure 1B, the PET nanocomposites exhibited similar absorption bands of pure PET, which were observed at 1715 (C=O), 1454 (CH<sub>2</sub>), 1407 (aromatic ring), 1247 (C-O), 1101 (O=CH<sub>2</sub>), 1018 (aromatic ring), and 723 cm<sup>-1</sup> (CH), respectively [56]. However, the stretching vibration peaks for the PET nanocomposites shifted from 1715, 1247, and 1101 to 1708, 1232, and 1085 cm<sup>-1</sup>, respectively, as compared to pure PET. This result indicated the existence of some interactions between the c-CNT and the PET matrix through hydrogen bonding formation, as shown in Figure 1C. Thus, it is expected that the enhanced interactions between the c-CNT and the PET matrix can lead to the good interfacial adhesion between them, resulting in the improvement in the overall mechanical properties of the PET nanocomposites due to the nanoreinforcing effect of the c-CNT.

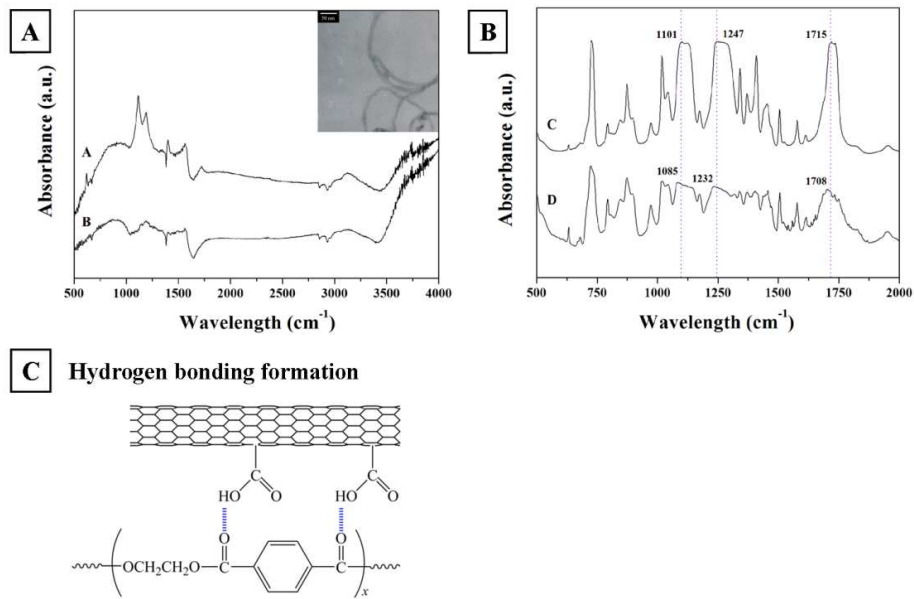


**Figure 1.** FT-IR spectra of (A) CNT and (B) the PET nanocomposites (a: c-CNT; b: pristine CNT; c: PET; and d: the PET nanocomposite containing 1.0 wt% of the c-CNT). The inset shows TEM images of the c-CNT after chemical modification. (C) Schematic showing possible interactions between the c-CNT and the PET matrix through hydrogen bonding formation. Reproduced with the permission from Ref. [46]. © 2010 Wiley Periodicals, Inc.

### 3.2. Thermal stability and thermal decomposition kinetics

TGA thermograms of the PET nanocomposites are shown in Figure 2, and their results are summarized in Table 1. The curve patterns of the PET nanocomposites are similar to that of pure PET, indicating that the features of the weight-loss for thermal decomposition of the PET nanocomposites may mostly stem from PET matrix. As shown in Table 1, the thermal decomposition temperatures, thermal stability factors, and residual yields of the PET nanocomposites increased with increasing the c-CNT content. The presence of the c-CNT can lead to the stabilization of the PET matrix, and good interfacial adhesion between the c-CNT and the PET may restrict the thermal motion of the PET molecules [57], resulting in the increased thermal stability of the PET nanocomposites. Shaffer and Windle [58] suggested that the thermal decomposition of CNT-filled polymer nanocomposites was retarded by high protecting effect of CNT against the thermal decomposition. In the PET nanocomposites, the effective function of the c-CNT as physical barriers to prevent the transport of volatile decomposed products in the polymer nanocomposites during thermal decomposition resulted in the enhanced thermal stability of the PET nanocomposites. Similar observation has been also reported that thermal stability of poly(ethylene 2,6-naphthalate) (PEN)/CNT nanocomposites was improved by physical barrier effects of CNT layers acting as effective thermal insulators in the PEN nanocomposites [40].

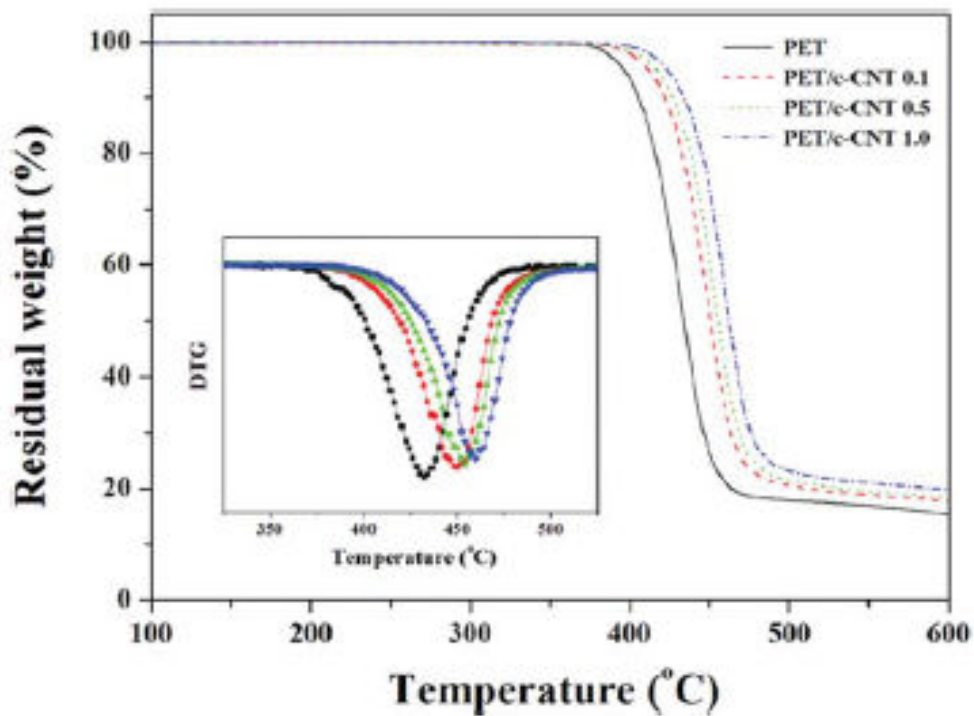


**Figure 2.** TGA thermograms of the PET nanocomposites. The inset shows the first derivative curves corresponding to TGA thermograms of the PET nanocomposite. Reproduced with the permission from Ref. [46]. © 2010 Wiley Periodicals, Inc.

Materials	$T_{di}^a$ (°C)	$T_{dm}^b$ (°C)	$A$	$K$	$IPDT^c$ (°C)	$W_R^d$ (%)
PET	387.8	432.1	0.7558	1.2627	573.8	15.7
PET/c-CNT 0.1	398.8	449.5	0.7803	1.2934	605.3	17.7
PET/c-CNT 0.5	402.7	452.9	0.7887	1.3025	615.3	18.3
PET/c-CNT 1.0	411.4	460.2	0.8017	1.3274	636.9	19.8

**Table 1.** Table 1. Effect of the c-CNT on the thermal stability of the PET nanocomposites. [<sup>a</sup> Initial decomposition temperatures at 2% of the weight-loss; <sup>b</sup> Decomposition temperature at the maximum rate of the weight-loss; <sup>c</sup> Integral procedure decomposition temperatures,  $IPDT = A K(T_f - T_i) + T_i$ , where  $A$  is the area ratio of total experimental curve divided by total TGA curves;  $K$  is the coefficient of  $A$ ;  $T_i$  is the initial experimental temperature, and  $T_f$  is the final experimental temperature [59]; <sup>d</sup> Residual yield in TGA thermograms at 600 °C under  $N_2$ ].

### 3.3. Rheological properties

As shown in Figure 3A, the  $|\eta^*|$  of the PET nanocomposites decreased with increasing frequency, indicating that the PET nanocomposites exhibited a non-Newtonian behavior over the whole frequency range measured. The shear thinning behavior of the PET nanocomposites resulted from the random orientation of entangled molecular chains in the polymer nanocomposites during the applied shear deformation. The  $|\eta^*|$  of the PET nanocomposites increased with the c-CNT content, and this effect was more pronounced at low frequency than at high frequency, indicating the formation of the interconnected or network-like struc-

tures in the PET nanocomposites as a result of nanotube-nanotube and nanotube-polymer interactions. In addition, the PET nanocomposites exhibited higher  $|\eta^*|$  values and more distinct shear thinning behavior as compared to pure PET, suggesting that better dispersion of the c-CNT or stronger interactions between the nanotubes and the polymer matrix [60]. The increase in the  $|\eta^*|$  of the PET nanocomposites with the introduction of the c-CNT was closely related to the increase in the storage modulus of the PET nanocomposites, which will be described in the following section. As shown in Figure 3B, the  $|\eta^*|$  of the PET nanocomposites decreased with increasing temperature. The temperature had little effect on the  $|\eta^*|$  of the PET nanocomposites at lower frequency, while at higher frequency, the rheological properties of the PET nanocomposites were affected by the temperature, and the  $|\eta^*|$  values of the PET nanocomposites decreased significantly with increasing temperature. This result indicated the enhancement in the flow behavior of the PET nanocomposite melts with increasing temperature.

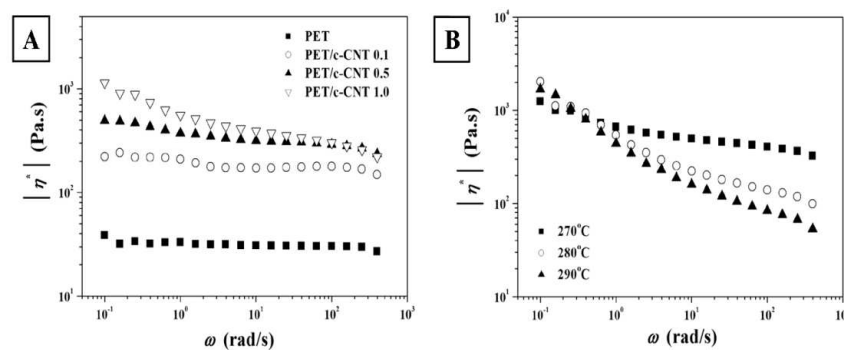


**Figure 3.** Complex viscosity of (A) the PET nanocomposites with the c-CNT content, and (B) the PET nanocomposites containing 1.0 wt% of the c-CNT at different temperatures as a function of frequency. Reproduced with the permission from Ref. [46]. © 2010 Wiley Periodicals, Inc.

The storage modulus ( $G'$ ) and loss modulus ( $G''$ ) of the PET nanocomposites as a function of frequency are shown in Figure 4. The storage and loss moduli of the PET nanocomposites increased with increasing frequency and c-CNT content and this effect was more pronounced at low frequency than at high frequency. This feature may be explained by the fact that the interactions between the nanotubes-nanotube and nanotube-polymer with the introduction of the c-CNT can lead to the formation of interconnected or network-like structures in the polymer nanocomposites [36, 53]. Furthermore, the values of  $G'$  and  $G''$  of the PET nanocomposites were higher than those of pure PET over the whole frequency range measured, and this enhancing effect was more pronounced at low frequency than at high frequency. The non-terminal behavior observed in the PET nanocomposites at low frequency, which was similar to the relaxation behavior of typical filled-polymer composite system [61], was related to the variation of the terminal slope of the flow curves based on the power-law equations:  $|\eta^*| \approx \omega^{-n}$  and  $G' \approx \omega^{-m}$  (where  $\omega$  is the frequency,  $n$  is the shear-thinning exponent, and  $m$  is the relaxation exponent) [62]. The variations of the shear-thinning exponent and relaxation exponent of the PET nanocomposites are shown in Figure 5. As com-

pared to pure PET, the lower shear thinning exponent of the PET nanocomposites indicated the significant dependence of shear-thinning behavior of the PET nanocomposites on the presence of the c-CNT, resulting from the increased interfacial interactions between the c-CNT and the PET as well as good dispersion of the c-CNT in the PET matrix. In addition, the decrease in the relaxation exponent of the PET nanocomposite with increasing the c-CNT content may be attributed to the formation of interconnected or network-like structures in the PET nanocomposites, resulting in the pseudo solid-like behavior of the PET nanocomposites. Similar non-terminal low frequency rheological behavior has been observed in ordered block copolymers, smectic liquid-crystalline small molecules, polymer/silicate nanocomposites, and CNT/polycarbonate composites [63–66]

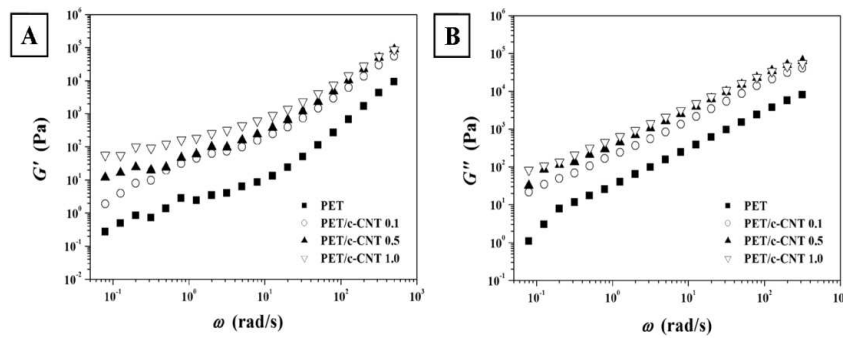


**Figure 4.** A) Storage modulus ( $G'$ ) and (B) loss modulus ( $G''$ ) of the PET nanocomposites as a function of frequency. Reproduced with the permission from Ref. [46]. © 2010 Wiley Periodicals, Inc.

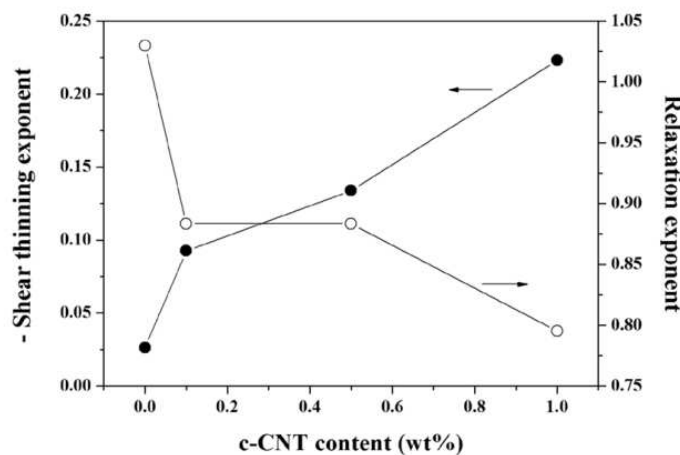


**Figure 5.** Variations of the shear thinning exponent and relaxation exponent of the PET nanocomposites with the c-CNT content. Reproduced with the permission from Ref. [46]. © 2010 Wiley Periodicals, Inc.

### 3.4. Morphology and mechanical properties

Pristine CNT typically tends to bundle together and to form some agglomeration due to the intrinsic van der Waals attractions between the individual nanotubes in combination with high aspect ratio and large surface area, making it difficult for CNT to disperse in the polymer matrix. In this study, the chemical modification was performed to achieve the enhanced adhesion between CNT and polymer matrix as well as good dispersion state of CNT. TEM image of the PET nanocomposites containing 0.1 wt% of the c-CNT is shown in Figure 6A. The c-CNT exhibited less entangled structures due to the functional groups formed on the nanotube surfaces via chemical modification as compared to pristine CNT (refer Figure 1), and the c-CNT was well dispersed in the PET matrix. SEM image of the fracture surfaces of the PET nanocomposites containing 1.0 wt% of the c-CNT is shown in Figure 6B. It can be observed that some nanotubes were broken with their two ends still embedded in the PET matrix and other nanotubes were bridging the local microcracks, which may delay the failure of the polymer nanocomposites [67]. This result indicates good wetting and adhesion of the c-CNT with the PET matrix. Similar observation has been reported that the presence of fractured tubes, along with the matrix still adhered to the fractured tubes matrix in terms of a crack interacting with the nanotube reinforcement could increased the elastic modulus and ultimate strength of CNT/polystyrene composites [68]. In the PET nanocomposites, the c-CNT stabilized their dispersion by good interactions with the PET matrix, resulting from the interfacial interactions of the -COOH groups at the c-CNT and the C=O groups in the PET macromolecular chains through hydrogen bonding formation due to the functional groups onto the nanotube surfaces induced effectively via chemical modification as illustrated in Figure 1C. This enhanced interfacial adhesion between the c-CNT and the PET matrix may be considered as the evidence for efficient load transfer from the polymer matrix to the nanotubes, thus leading to the nanoreinforcing effects of the c-CNT on the improvement in the mechanical properties of the PET nanocomposites

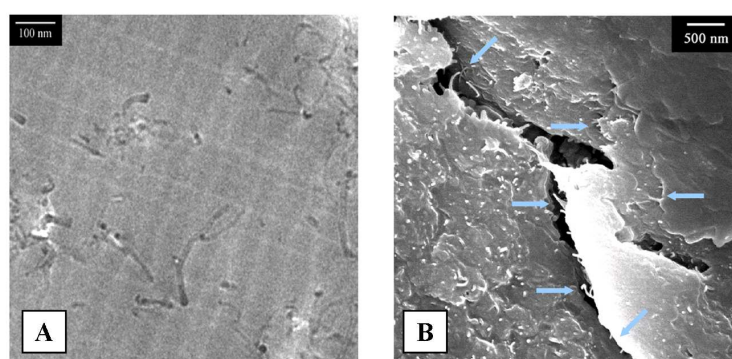


**Figure 6.** TEM image of (a) the PET nanocomposites containing 0.1 wt% of the c-CNT and (b) SEM image of the fracture surfaces of the PET nanocomposites containing 1.0 wt% of the c-CNT. The arrows indicates that the nanotubes were to be broken with their ends still embedded in the PET matrix or they were bridging the local micro-cracks in the nanocomposites, suggesting good wetting with the matrix and enhanced adhesion between the nanotubes and the matrix, thus being favorable to efficient load transfer form the polymer matrix to the nanotubes. Reproduced with the permission from Ref. [46]. © 2010 Wiley Periodicals, Inc.

The mechanical properties of the PET nanocomposites with the c-CNT are shown in Figure 7A. The tensile strength ( $\sigma$ ) and tensile modulus ( $E$ ) of the PET nanocomposites increased significantly with increasing the c-CNT content due to the nanoreinforcing effect of the c-CNT with high aspect ratio. As illustrated in Figure 1C, possible interactions between the carboxylic acid groups of the c-CNT and the ester groups in PET macromolecular chains through hydrogen bonding formation results in the enhanced interfacial adhesion between them as well as good dispersion of the c-CNT in the PET matrix, thus being more favorable to more effective load transfer from the polymer matrix to the nanotubes, and lead to the substantial improvement in the mechanical properties of the PET nanocomposites. The elongation at break ( $E_b$ ) of the PET nanocomposites decreased with the introduction of CNT (Table 2), which may be attributed to the increase in the stiffness of the PET nanocomposites by the c-CNT and the micro-voids formed around the nanotube during the tensile testing [40, 41]. However, the PET nanocomposites containing the c-CNT exhibited higher  $E_b$  than in the case of pristine CNT, resulting from the enhanced interfacial interactions between the c-CNT and the PET as well as the good dispersion of the c-CNT in the PET matrix. Meng et al. [69] reported that modified CNT/polyamide (PA) nanocomposites showed higher tensile strength, tensile modulus, and elongation at break than those of pristine CNT/PA nanocomposites because of uniform dispersion and good interfacial adhesion in the modified CNT/PA nanocomposites.

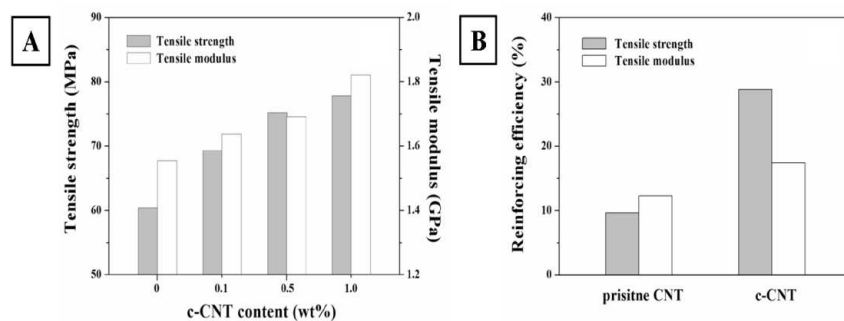


**Figure 7.** A) Mechanical properties of the PET nanocomposites and (B) the reinforcing efficiency of pristine CNT and the c-CNT on the mechanical properties of the PET nanocomposites containing 1.0 wt% of the CNT. Reinforcing efficiency (%) =  $[(M_c - M_m)/M_m] \times 100$ , where  $M_c$  and  $M_m$  represent the mechanical properties, such as tensile strength and tensile modulus, of the PET nanocomposites and pure PET, respectively. Reproduced with the permission from Ref. [46]. © 2010 Wiley Periodicals, Inc.

Materials	$\sigma^a$ (MPa)	$E$ (GPa)	$E_b$ (%)
PET	60.4 ± 1.8	1.55 ± 0.072	174 ± 19
PET/c-CNT 1.0	77.8 ± 3.2	1.82 ± 0.028	96 ± 12
PET/p-CNT 1.0 <sup>a</sup>	66.2 ± 1.2	1.74 ± 0.031	81 ± 15

**Table 2.** Mechanical properties of the PET nanocomposites. [<sup>a</sup> The p-CNT represents pristine CNT without chemical modification].

For characterizing the effect of the c-CNT on the mechanical properties of the PET nanocomposites, it is also very instructive to compare the reinforcing efficiency of the c-CNT for a given content in the PET nanocomposites. The reinforcing efficiency is defined as the normalized mechanical properties of the PET nanocomposites with respect to those of pure PET as follows:

Reinforcing efficiency (%)

$$= \frac{M_c - M_m}{M_m} \times 100$$

where  $M_c$  and  $M_m$  represent the mechanical properties, including tensile strength and tensile modulus of PET nanocomposites and pure PET, respectively. As shown in Figure 7B, the enhancing effect of the mechanical properties for the PET nanocomposites was more significant in the PET nanocomposites containing the c-CNT than in the case of pristine CNT. This result indicated that the introduction of the c-CNT into the PET matrix was more effective in improving the mechanical properties of the PET nanocomposites as compared to pristine CNT. The incorporation of the c-CNT into the PET matrix resulted in the increased interfacial adhesion between the c-CNT and the PET matrix, thus being favorable to more efficient load transfer from the polymer matrix to the nanotubes. Thus, the enhanced interfacial adhesion between the c-CNT and the PET as well as good dispersion of the c-CNT result in the improvement in the overall mechanical properties of the PET nanocomposites.

### 3.5. Non-isothermal crystallization behavior

The incorporation of the c-CNT had little effect on the melting temperatures of the PET nanocomposites, whereas the glass transition temperature of the PET nanocomposites increased with the introduction of the c-CNT, resulting from the hindrance of the segmental motions of the PET macromolecular chains by the c-CNT. As shown in Figure 8A, the crystallization temperatures of the PET nanocomposites significantly increased by incorporating the c-CNT and this enhancing effect was more pronounced at lower content. This result indicated the efficiency of the c-CNT as strong nucleating agents for the PET crystallization. As the c-CNT content increased, the decrease in the  $\Delta T$  for crystallization as well as the increase in the  $T_{mc}$  of the PET nanocomposites (Table 3) suggested that a very small quantity of the c-CNT acted as effective nucleating agents in PET, enhancing the crystallization of the PET nanocomposites with the presence of the c-CNT. The non-isothermal crystallization curves of the PET nanocomposites at various cooling rates are shown in Figure 8B. As the cooling rate increased, the crystallization peak temperature range becomes broader and shifts to lower temperatures, indicating that the lower the cooling rate, the earlier crystallization occurs. The PET nanocomposites exhibited higher peak temperature and lower overall crystallization time at a given cooling rate, as compared to pure PET. Homogeneous nucleation started spontaneously below the melting temperature and required longer times, whereas heterogeneous nuclei formed as soon as samples reached the crystallization temperature [70]. As the crystallization of polymer nanocomposites proceeds through heteroge-

neous nucleation, the introduction of the c-CNT increased the PET crystallization because of high nucleation induced by the c-CNT. Similar observations have been reported that the crystallization of CNT/polymer nanocomposites was accelerated by the presence of CNT through heterogeneous nucleation [35, 38, 40-43].

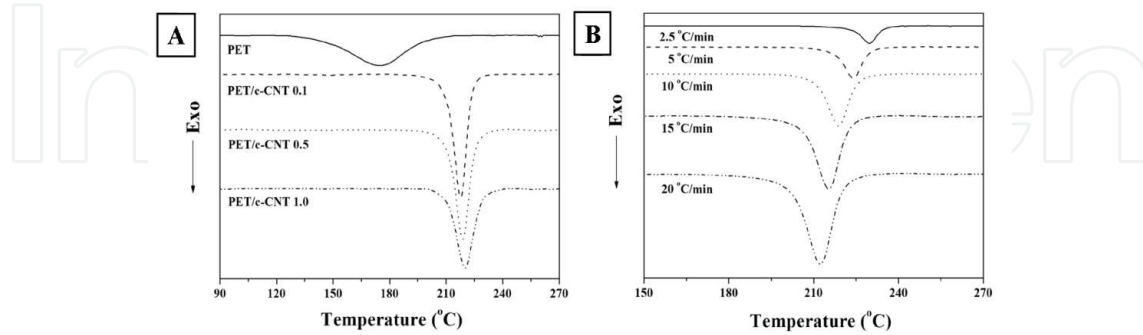


**Figure 8.** A) DSC cooling traces of the PET nanocomposites at a cooling rate of 10 °C/min and (B) the non-isothermal crystallization curves of the PET nanocomposites containing 0.5 wt% of the c-CNT at various cooling rates. Reproduced with the permission from Ref. [46]. © 2010 Wiley Periodicals, Inc.

Materials	$T_g$ (°C)	$T_m$ (°C)	$T_c$ (°C)	$\Delta T^a$ (°C)
PET	84.4	255.4	193.7	61.7
PET/c-CNT 0.1	90.4	255.3	218.6	36.7
PET/c-CNT 0.5	91.3	255.2	219.0	36.2
PET/c-CNT 1.0	92.0	255.9	219.6	36.3

**Table 3.** Table 3. Thermal behaviour of PET nanocomposites [<sup>a</sup> The values obtained from the DSC heating traces at 10 °C/min; <sup>b</sup> The crystallization temperatures measured from the DSC cooling traces at 10 °C/min; <sup>c</sup> The degree of supercooling,  $\Delta T = T_m - T_{mc}$ ]

During the non-isothermal crystallization, the relative degree of crystallinity,  $X(T)$ , with temperature and time for the PET nanocomposites at various cooling rates are shown in Figure 9. The crystallization of the PET nanocomposites occurred at higher temperature and over a longer time with decreasing cooling rate, suggesting that crystallization may be controlled by nucleation [71]. As the cooling rate increased, the time for completing crystallization was decreased and the  $X(T)$  values of the PET nanocomposites were higher than that of pure PET. The variations of the crystallization peak temperature ( $T_p$ ) and the crystallization half-time ( $t_{0.5}$ ) of the PET nanocomposites are shown in Figure 10. The  $T_p$  of the PET nanocomposites were higher than that of pure PET at a given cooling rate, while the  $t_{0.5}$  were lower than that of pure PET. This result suggested that the introduction of the c-CNT increased the crystallization rate of the PET nanocomposites by its effective function as strong nucleating agents for enhancing the PET crystallization. This enhancing effect of the crystallization rate induced by the c-CNT may be attributed to the interactions between the carboxylic acid groups on the surface of the c-CNT and the PET macromolecular chains as well as

the physical adsorption of PET molecules onto the surface of the c-CNT, resulting in the enhancement of the crystallization rate of the PET nanocomposites. Similar observation has been reported that the introduction of carboxylated CNT increased more efficiently the crystallization rate of polyamide [72]

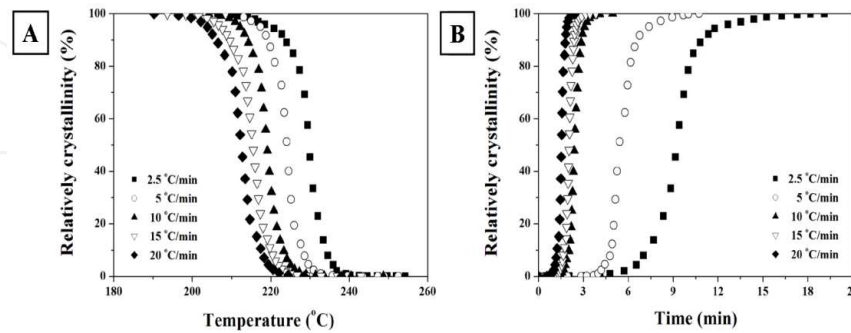


**Figure 9.** Relative degree of crystallinity of the PET nanocomposites containing 0.5 wt% of the c-CNT with (A) the temperature and (B) the time at various cooling rates. Reproduced with the permission from Ref. [46]. © 2010 Wiley Periodicals, Inc.

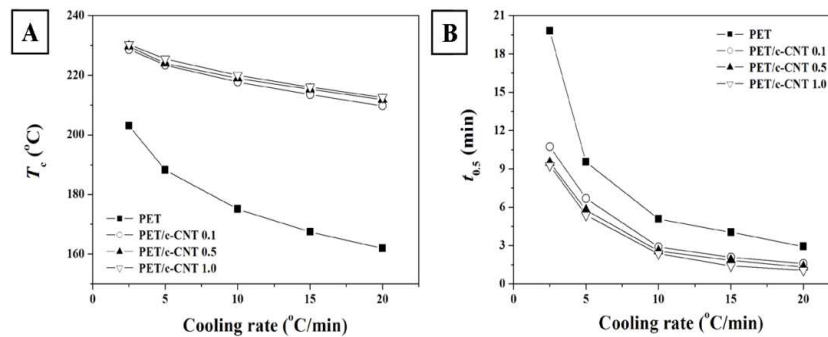


**Figure 10.** A) Crystallization temperatures ( $T_c$ ) and (B) crystallization half-time ( $t_{0.5}$ ) of the PET nanocomposites as a function of cooling rate during the non-isothermal crystallization. The crystallization half-time ( $t_{0.5}$ ) can be defined as the time taken to complete half of the non-isothermal crystallization process, i.e., the time required to attain a relative degree of crystallinity of 50%. Reproduced with the permission from Ref. [46]. © 2010 Wiley Periodicals, Inc.

On the basis of the  $T_p$  values obtained from the non-isothermal crystallization curves, the fastest crystallization time ( $t_{max}$ ) at various cooling rates ( $a$ ) can be determined and their results are summarized in Table 4. The  $t_{max}$  represents the time from the onset temperature ( $T_0$ ) to the peak temperature ( $T_p$ ) of the crystallization and can be expressed by the relationship of  $t_{max} = (T_0 - T_c)/a$  [73]. At a given cooling rate, the  $t_{max}$  values of the PET nanocomposites decreased with the introduction of the c-CNT. This result indicated that the nucleation effect by the c-CNT was significant even with a very small quantity of the c-CNT, providing possible evidence of the enhancement of the crystallization rate for the PET nanocomposites due to high nucleation induced by the c-CNT. In addition, the effect of the c-

CNT on the non-isothermal crystallization rate of the PET nanocomposites was characterized by means of the crystallization rate constant (CRC) suggested by Khanna [74]. The CRC can be calculated from the slope of the plots of the cooling rate versus the crystallization temperature plot, i.e.,  $CRC = \Delta a / \Delta T_c$ , meaning that the larger the CRC, the faster the crystallization rate. The CRC value of pure PET in this study was similar to those reported by Khanna [74], who found the CRC values of PET in the range of 30~60/h, depending on the molecular weight and the processing method. As shown in Figure 11A, the CRC values of the PET nanocomposites significantly increased with the introduction of the c-CNT, indicating the higher crystallization rate of the PET nanocomposites as compared to pure PET because of high nucleation effect induced by the c-CNT. In addition, the CRC values of the PET nanocomposites significantly increased with the addition of 0.1 wt% of the c-CNT, and increased slightly with further addition of the c-CNT. This result revealed that the acceleration of the non-isothermal crystallization for the PET nanocomposites was not directly proportional to the increase in the c-CNT content and that the enhancement of the crystallization rate of the PET nanocomposites induced by the c-CNT could not be described by means of simple linear regression method, implying the complex mechanism of the non-isothermal crystallization process in the presence of the c-CNT. The enhanced interfacial interactions between the functional groups induced on the surface of the c-CNT and the PET as well as the strong nucleation effect of the c-CNT could increase the crystallization rate of the PET nanocomposites

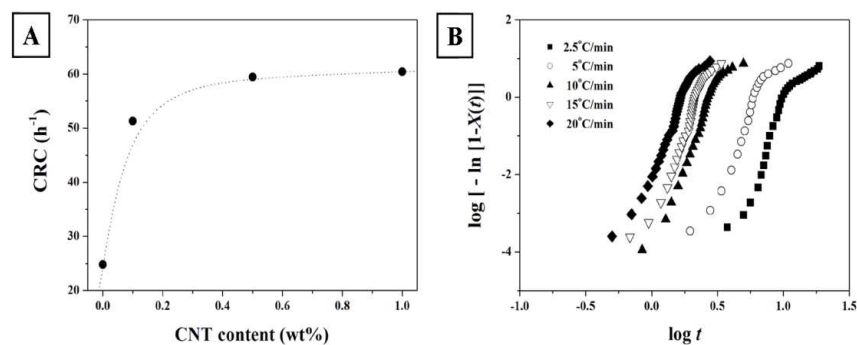


**Figure 11.** A) Crystallization rate constant (CRC) for the PET nanocomposites with the c-CNT content and (B) the modified Avrami plots of the PET nanocomposites containing 0.1 wt% of the c-CNT during the non-isothermal crystallization. Reproduced with the permission from Ref. [46]. © 2010 Wiley Periodicals, Inc.

The modified Avrami equation [75, 76] is in common use to characterize the non-isothermal crystallization kinetics, and can be expressed as:

$$1 - X(t) = \exp(-Z_t t^n)$$

where  $X(t)$  is the relative degree of crystallinity;  $Z_t$  is the crystallization rate parameter involving the nucleation and growth rate parameters;  $t$  is the crystallization time, and  $n$  is the Avrami constant depending on the type of nucleation and growth process. The kinetic parameters such as  $Z_t$  and  $n$  explicit physical meanings for the isothermal crystallization,

while in the non-isothermal crystallization their physical meaning does not have the same significance due to constant changes in the temperature, influencing the nucleation and crystal growth. On the basis of the non-isothermal character of the process suggested by Jeziorny [77], the rate parameter ( $Z_c$ ) should be corrected by assuming the cooling rate to be constant or approximately constant, according to the relationship of  $\log Z_c = \log Z_t / a$  (where  $a$  is the cooling rate). The plots of  $\log[-\ln\{1 - X(t)\}]$  versus  $\log t$  for the PET nanocomposites are shown in Figure 11B. The kinetic parameters such as  $n$  and  $Z_t$  can be determined from the slope and intercept of the plot of  $\log[-\ln\{1 - X(t)\}]$  versus  $\log t$ . The kinetic parameters for the non-isothermal crystallization of the PET nanocomposites estimated from the kinetic data selected in the linear region are summarized in Table 4. The  $n$  values were in the range of 3.21~3.56 for pure PET, whereas 4.14~6.29 for the PET nanocomposites, depending on the cooling rate and the c-CNT content. The PET nanocomposites exhibited values of  $n$  higher than 4, suggesting that the mechanism of the non-isothermal crystallization of the PET nanocomposites was very complicated and the c-CNT significantly influenced the non-isothermal crystallization behavior, leading to the fact that the incorporation of the c-CNT into the PET matrix could change the non-isothermal crystallization of the PET nanocomposites. As the cooling rate increased, the  $t_{0.5}$  values decreased and the  $Z_c$  values increased for the PET nanocomposites in comparison with pure PET. In addition, the PET nanocomposites exhibited higher  $Z_c$  and lower  $t_{0.5}$  values than those of pure PET at a given cooling rate. This result revealed that the c-CNT dispersed in the PET matrix could induce heterogeneous nucleation and enhance the rate of the non-isothermal crystallization of the PET nanocomposites. The introduction of the c-CNT into the PET matrix can lead to faster crystallization kinetics of the PET nanocomposites, and significantly influence the non-isothermal crystallization process involving the nucleation and the crystal growth.

### 3.6. Nucleation activity and crystallization activation energy

The nucleation activity is a factor by which the work of three dimensional nucleation decreases with the addition of a foreign substrate [78], the nucleation activity of different substrates can be estimated from the relationship of  $\log a = A - B/2.3\Delta T_p^2$  (where  $a$  is the cooling rate;  $A$  is a constant;  $\Delta T_p$  is the degree of supercooling, and  $B$  is parameter related to three dimensional nucleation) [35, 40, 78]. The  $B$  values were obtained from the slope of the plot of  $\log a$  versus  $1/T_p^2$  as shown in Figure 12A, and then the nucleation activity ( $\phi$ ) can be calculated from the relationship of  $\phi = B^*/B^0$  (where  $B^0$  and  $B^*$  are the values of  $B$  for homogeneous and heterogeneous nucleation, respectively). The value of 0 implied strong nucleation activity and that of 1 implied inert nucleation activity. The calculated values in the PET nanocomposites were found to be 0.227, 0.231, and 0.211, respectively. This result demonstrates that a very small quantity of the c-CNT can act as excellent nucleating agents for the PET nanocomposites during the non-isothermal crystallization, which was corresponded well with the results for the non-isothermal crystallization kinetics of the PET nanocomposites. The incorporated c-CNT in the PET matrix exhibits much higher nucleation activity than any other nanoreinforcing filler reported to date, with even a very small quantity of the c-CNT.

Materials	Cooling rate (°C/min)	$Z_c$	$N$	$t_{max}$ (min)
PET	2.5	$4.54 \times 10^{-6}$	3.55	12.46
	5	$2.27 \times 10^{-3}$	3.33	7.87
	10	$5.70 \times 10^{-2}$	3.56	4.66
	15	$1.74 \times 10^{-1}$	3.37	3.50
	20	$2.99 \times 10^{-1}$	3.21	2.73
PET/c-CNT 0.1	2.5	$2.01 \times 10^{-2}$	5.09	10.02
	5	$2.27 \times 10^{-1}$	4.93	5.76
	10	$4.89 \times 10^{-1}$	5.56	3.00
	15	$7.46 \times 10^{-1}$	5.83	1.91
	20	$8.31 \times 10^{-1}$	5.36	1.43
PET/c-CNT 0.5	2.5	$1.95 \times 10^{-2}$	5.02	9.86
	5	$2.14 \times 10^{-1}$	4.14	5.70
	10	$5.57 \times 10^{-1}$	5.71	2.99
	15	$7.02 \times 10^{-1}$	6.29	1.85
	20	$8.52 \times 10^{-1}$	6.17	1.28
PET/c-CNT 1.0	2.5	$1.94 \times 10^{-2}$	4.87	9.72
	5	$2.93 \times 10^{-1}$	4.78	5.51
	10	$6.01 \times 10^{-1}$	5.89	2.96
	15	$8.05 \times 10^{-1}$	4.59	1.87
	20	$9.09 \times 10^{-1}$	5.13	1.30

**Table 4.** Kinetic parameters of PET nanocomposites during the non-isothermal crystallization

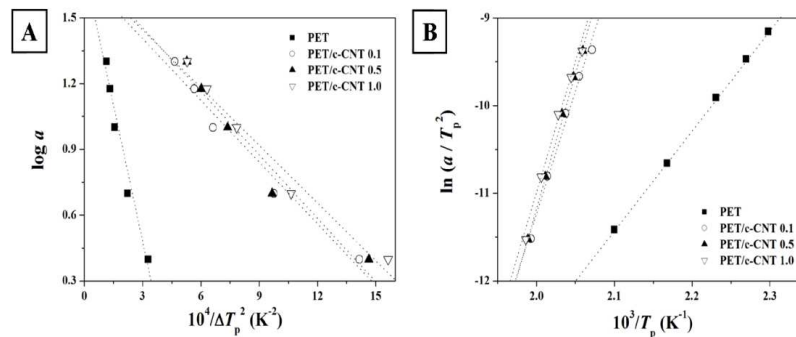


**Figure 12.** Plots of  $\log a$  versus of  $1/\Delta T_p^2$ , for the PET nanocomposites. Using the slope of the plot of  $\log a$  versus of  $1/\Delta T_p^2$ , the nucleation activity ( $n$ ) can be calculated from the relationship of  $n = B^*/B^0$  and (b) Plots of  $\ln(a/T_p^2)$  versus  $1/T_p$ , for the PET nanocomposites. The slopes of the plots of  $\ln(a/T_p^2)$  versus  $1/T_p$ , provide an estimate of the activation energy for non-isothermal crystallization of the PET nanocomposites. Reproduced with the permission from Ref. [46]. © 2010 Wiley Periodicals, Inc.

The activation energy for the non-isothermal crystallization can be derived from the combination of the cooling rate and the crystallization peak temperature, suggested by Kissinger [79]. The  $\Delta E_a$  values of the PET nanocomposites were obtained from the slope of the plot of

$\ln(a/T_p^2)$  versus  $1/T_p$  as shown in Figure 12B. The calculated  $\Delta E_a$  values of the PET nanocomposites were found to be 231.1, 255.9, and 248.9 kJ/mol, respectively, and they were higher than that of pure PET ( $\Delta E_a = 5.3$  kJ/mol). This result indicated that the introduction of the c-CNT probably reduced the transportation ability of polymer chains in the PET nanocomposites during the non-isothermal crystallization [80], leading to the increase in the  $\Delta E_a$  values. However, the addition of 1 wt% of the c-CNT induced more heterogeneous nucleation, and could lead to the slight decrease in the  $\Delta E_a$  value of the PET nanocomposite during the non-isothermal crystallization. Kim et al. [35, 40] studied the unique nucleation of multiwalled CNT and PEN nanocomposites during the non-isothermal crystallization and they suggested that the introduced CNT could perform two functions in the PEN nanocomposites: CNT acted as good nucleating agents, thus accelerating the non-isothermal crystallization of the PEN nanocomposites, and CNT also adsorbed the PEN molecular segments and restricted the movement of chain segments, thereby making crystallization difficult. Consequently, the PEN molecular segments require more energy to rearrange, leading to the increase in the activation energy for the non-isothermal crystallization

#### 4. Summary and Outlook

This chapter describes the fabrication and characterization of poly(ethylene terephthalate) (PET) nanocomposites containing modified carbon nanotube (CNT). The PET nanocomposites reinforced with a very small quantity of the c-CNT were prepared by simple melt blending in a twin-screw extruder to create high performance polymer nanocomposites for practical applications in a broad range of industries. The carboxylic acid groups effectively induced on the surfaces of the c-CNT via chemical modification can significantly influence the mechanical and rheological properties, thermal stability, and non-isothermal crystallization behavior of the PET nanocomposites. Morphological observation revealed that the c-CNT was well dispersed in the PET matrix and enhanced the interfacial adhesion between the nanotubes and the PET matrix. The enhancement of thermal stability of the PET nanocomposites resulted from the physical barrier effect of the c-CNT against the thermal decomposition. The incorporation of the c-CNT into the PET matrix increased the shear thinning nature of the PET nanocomposites, and the non-terminal behavior observed in the PET nanocomposites was attributable to the nanotube-nanotube and nanotube-polymer interactions. The improvement in the mechanical properties of PET nanocomposites with the introduction of the c-CNT resulted from the enhanced interfacial interactions between the c-CNT and the PET as well as good dispersion of the c-CNT in the PET matrix. The variations of the nucleation activity and the crystallization activation energy of the PET nanocomposites reflected the enhancement of crystallization of the PET nanocomposites effectively induced by a very small quantity of the c-CNT. The incorporation of the c-CNT into the PET matrix has a significant effect on the non-isothermal crystallization kinetics of the PET nanocomposites in that the c-CNT dispersed in the PET matrix can effectively act as strong nucleating agents and lead to the enhanced crystallization of the PET nanocomposites through heterogeneous nucleation. The uniform dispersion of modified CNT and strong interfacial

adhesion or intimate contact between the nanotubes and the polymer matrix can lead to more effect load transfer from the polymers to the nanotubes, resulting in the substantial enhancement of mechanical properties of PET/CNT nanocomposites even with a very small quantity of modified CNT. Future development of PET/CNT nanocomposites for targeted applications in a broad range of industry will be performed by balancing high performance against multiple functionalities and manufacturing cost.

## Acknowledgements

Authors thank Mr. H. J. Choi, Mr. C. S. Kang, and Mr. D. K. Kim for their assistance in part with the experiment and characterization of PET nanocomposites in this study.

## Author details

Jun Young Kim<sup>1\*</sup> and Seong Hun Kim<sup>2</sup>

\*Address all correspondence to: junykim74@hanmail.net

1 Corporate Research & Development Center, Samsung SDI Co. Ltd., Republic of Korea

2 Department of Organic & Nano Engineering, Hanyang University,, Republic of Korea

## References

- [1] Imai, Y., Nishimura, S., Abe, E., Tateyama, H., Abiko, A., Yamaguchi, A., & Taguchi, H. (2002). High-Modulus Poly(ethylene terephthalate)/Expandable Fluorine Mica Nanocomposites with a Novel Reactive Compatibilizer. *Chem. Mater.*, 14, 477-479.
- [2] Jeol, S., Fenouillot, F., Rousseau, A., & Varlot, K. M. (2007). Drastic Modification of the Dispersion State of Submicron Silica During Biaxial Deformation of Poly(ethylene terephthalate). *Macromolecules*, 40, 3229-3237.
- [3] Giannelis, E.P. (1996). Polymer Layered Silicate Nanocomposites. *Adv. Mater.*, 8, 29-35.
- [4] Kim, J. Y., Seo, E. S., Kim, S. H., & Kikutani, T. (2003). Effects of Annealing on Structure and Properties of TLCP/PEN/PET Ternary Blend Fibers. *Macromol. Res.*, 11, 62-68.
- [5] Kim, J. Y., Kim, O. S., Kim, S. H., & Jeon, H. Y. (2004). Effects of Electron Beam Irradiation on Poly(ethylene 2,6-naphthalate)/Poly(ethylene terephthalate) Blends. *Polym. Eng. Sci.*, 44, 395-405.

- [6] Kim, J. Y., Kim, S. H., & Kikutani, T. (2004). Fiber Property and Structure Development of Polyester Blend Fibers Reinforced with a Thermotropic Liquid-Crystal Polymer. *J. Polym. Sci. Part B: Polym. Phys.*, 42, 395-403.
- [7] Kim, J. Y., & Kim, S. H. (2005). Situ Fibril Formation of Thermotropic Liquid Crystal Polymer. *Polyesters Blends. J. Polym. Sci. Part B: Polym. Phys.*, 43, 3600-3610.
- [8] Kim, J. Y., Kang, S. W., Kim, S. H., Kim, B. C., & Lee, J. G. (2005). Deformation Behavior and Nucleation Activity of a Thermotropic Liquid-crystalline Polymer. *Poly(butylene terephthalate)-Based Composites. Macromol. Res.*, 13, 19-29.
- [9] Kim, J. Y., & Kim, S. H. (2006). Structure and Property Relationship of Thermotropic Liquid Crystal Polymer and Polyester Composite Fibers. *J. Appl. Polym. Sci.*, 99, 2211-2219.
- [10] Kim, J. Y., & Kim, S. H. (2006). Influence of viscosity ratio on processing and morphology of thermotropic liquid crystal polymer-reinforced poly(ethylene 2,6-naphthalate) blends. *Polym. Int.*, 55, 449-455.
- [11] Kim, J. Y., Kim, D. K., & Kim, S. H. (2009). Thermal Decomposition Behavior of Poly(ethylene 2,6-naphthalate)/Silica Nanocomposites. *Polym. Compos*, 30, 1779-1787.
- [12] Iijima, S. (1991). Helical Microtubes of Graphitic Carbon. *Nature*, 354, 56-58.
- [13] Dresselhaus, M. S., Dresselhaus, G., & Avouris, P. H. (2001). Carbon Nanotubes. *Synthesis, Structure, Properties, and Applications*, Berlin, Springer.
- [14] Shonaike, G. O., & Advani, S. G. (2003). *Advanced Polymeric Materials*, New York, CRC Press.
- [15] Thostenson, E. T., Ren, Z., & Chou, T. W. (2001). Advanced in the Science and Technology of Carbon Nanotubes and their Composites : A Review. *Compos. Sci. Technol.*, 61, 1899-1912.
- [16] Goze, C., Bernier, P., Henrard, L., Vaccarini, L., Hernandez, E., & Rubio, A. (1999). Elastic and Mechanical Properties of Carbon Nanotubes. *Synth. Metals*, 103, 2500-2501.
- [17] Yao, Z., Zhu, C. C., Cheng, M., & Liu, J. (2001). Mechanical Properties of Carbon Nanotube by Molecular Dynamics Simulation. *Comput. Mater. Sci.*, 22, 180-184.
- [18] Yu, M. F., Files, B. S., Arepalli, S., & Ruoff, R. S. (2000). Tensile Loading of Ropes of Single Wall Carbon Nanotubes and their Mechanical Properties. *Phys. Rev. Lett.*, 84, 5552-5555.
- [19] Yu, M. F., Lourie, O., Dyer, M. J., Moloni, K., Kelly, T. F., & Ruoff, R. S. (2000). Strength and Breaking Mechanism of Multiwalled Carbon Nanotubes Under Tensile Load. *Science*, 287, 637-640.
- [20] Frank, S., Poncharal, P., Wang, Z. L., & De Heer, W. A. (1998). Carbon Nanotube Quantum Resistors. *Science*, 280, 1744-1746.

- [21] Ebbesen, T. (1997). Carbon Nanotubes: *Preparation and Properties*, New York, CRC Press.
- [22] Schadler, L. S., Giannaris, S. C., & Ajayan, P. M. (1998). Load Transfer. *Carbon Nanotube Epoxy Composites. Appl. Phys. Lett.*, 73, 3842-3844.
- [23] Ajayan P.M., . (1999). Nanotubes from Carbon. *Chem. Rev.*, 99, 1787-1800.
- [24] Bokobza, L. (2007). Multiwall Carbon Nanotube Elastomeric Composites. *Polymer*, 48, 4907-4920.
- [25] Paul, D. R., & Robesson, L. M. (2008). Polymer Nanotechnology: *Nanocomposites. Polymer*, 49, 3187-3204.
- [26] De Heer, W. A. (1995). Chatelain A., Ugarte D. Carbon Nanotube Field-emission Electron Source. *Science*, 270, 1179-1180.
- [27] Wong, E. W., Sheehan, P. E., & Lieber, C. M. (1997). Nanobeam Mechanics: Elasticity, Strength, and Toughness of Nanorods and Nanotubes. *Science*, 277, 1971-1975.
- [28] Fan, S., Chapline, M. G., Franklin, N. R., Tomblor, T. W., Casell, A. M., & Dai, H. (1999). Self-oriented Regular Arrays of Carbon Nanotubes and Their Field Emission Properties. *Science*, 283, 512-514.
- [29] Kim, P., & Lieber, C. M. (1999). Nanotube Nanotweezers. *Science*, 286, 2148-2150.
- [30] Liu, C., Fan, Y. Y., Liu, M., Kong, H. T., & Cheng, H. M. (1999). Dresselhaus M.S. Hydrogen Storage in Single-walled Carbon Nanotubes at Room Temperature. *Science*, 286, 1127-1129.
- [31] Kong, J., Franklin, N., Zhou, C., Peng, S., Cho, J. J., & Dai, H. (2000). Nanotube Molecular Wires as Chemical Sensor. *Science*, 287, 622-625.
- [32] Ishihara, T., Kawahara, A., Nishiguchi, H., Yoshio, M., & Takita, Y. (2001). Effects of Synthesis Condition of Graphitic Nanocarbon Tube on Anodic Property of Li-ion Rechargeable Battery. *J. Power Sources*, 97(98), 129-132.
- [33] Alan, B., Dalton, A. B., Collins, S., Munoz, E., Razal, J. M., Ebron, V. H., Ferraris, J. P., Coleman, J. N., Kim, B. G., & Baughman, R. H. (2003). Super-tough Carbon Nanotube Fibres. *Nature*, 423, 703.
- [34] Wu, M., & Shaw, L. A. (2005). Novel Concept of Carbon-filled Polymer Blends for Applications in PEM Fuel Cell Bipolar Plates. *Int. J. Hydrogen Energy*, 30, 373-380.
- [35] Kim, J. Y., Park, H. S., & Kim, S. H. (2006). Unique Nucleation of Multiwalled Carbon Nanotube and Poly(ethylene 2,6-naphthalate) Nanocomposites During Non-isothermal Crystallization. *Polymer*, 47, 1379-1389.
- [36] Kim, J. Y., & Kim, S. H. (2006). Influence of Multiwall Carbon Nanotube on Physical Properties of Poly(ethylene 2,6-naphthalate) Nanocomposites. *J. Polym. Sci. Part B: Polym. Phys.*, 44, 1062-1071.

- [37] Kim, J. Y., Park, H. S., & Kim, S. H. (2007). Multiwall Carbon Nanotube-Reinforced Poly(ethylene terephthalate) Nanocomposites by Melt Compounding. *J. Appl. Polym. Sci.*, 103, 1450-1457.
- [38] Kim, J. Y., Han, S. I., & Kim, S. H. (2007). Crystallization Behavior and Mechanical Properties of Poly(ethylene 2,6-naphthalate)/Multiwall Carbon Nanotube Nanocomposites. *Polym. Eng. Sci.*, 47, 1715-1723.
- [39] Kim, J. Y., & Kim, S. H. (2008). Multiwall Carbon Nanotube Reinforced Polyester Nanocomposites. *Polyesters: Properties, Preparation and Applications*, New York, Nova Science Publishers, 33-107.
- [40] Kim, J. Y., Han, S. I., & Hong, S. (2008). Effect of Modified Carbon Nanotube on the Properties of Aromatic Polyester Nanocomposites. *Polymer*, 49, 3335-3345.
- [41] Kim, J.Y. (2009). The Effect of Carbon Nanotube on the Physical Properties of Poly(butylene terephthalate) Nanocomposite by Simple Melt Blending. *J. Appl. Polym. Sci.*, 112, 2589-2600.
- [42] Kim, J. Y., Kim, D. K., & Kim, S. H. (2009). Effect of Modified Carbon Nanotube on Physical Properties of Thermotropic Liquid Crystal Polyester Nanocomposites. *Eur. Polym. J.*, 45, 316-324.
- [43] Kim, J. Y., Han, S. I., Kim, D. K., & Kim, S. H. (2009). Mechanical Reinforcement and Crystallization Behavior of Poly(ethylene 2,6-naphthalate) Nanocomposites Induced by Modified Carbon Nanotube. *Composites: Part A*, 40, 45-53.
- [44] Kim, J. Y., Park, H. S., & Kim, S. H. (2009). Thermal Decomposition Behavior of Carbon Nanotube-Reinforced Poly(ethylene 2,6-naphthalate). *Nanocomposites. J. Appl. Polym. Sci.*, 113, 2008-2017.
- [45] Kim, J.Y. (2009). Carbon Nanotube-reinforced thermotropic Liquid Crystal Polymer Nanocomposites. *Materials*, 2, 1955-1974.
- [46] Kim, J. Y., Choi, H. J., Kang, C. S., & Kim, S. H. (2010). Influence of Modified Carbon Nanotube on Physical Properties and Crystallization Behavior of Poly(ethylene terephthalate) Nanocomposites. *Polym. Compos*, 31, 858-869.
- [47] Kim, J.Y. (2011). Aromatic Polyester Nanocomposites Containing Modified Carbon Nanotube. *Thermoplastic and Thermosetting Polymers and Composites.*, New York, Nova Science Publishers, 1-36.
- [48] Kim, J.Y. (2011). Poly(butylene terephthalate) Nanocomposites Containing Carbon Nanotube. *Advances in Nanocomposites: Synthesis, Characterization and Industrial Applications*, Rijeka, InTech, 707-726.
- [49] Wang, C., Guo, Z. X., Fu, S., Wu, W., & Zhu, D. (2004). Polymers Containing Fullerene of Carbon Nanotube Structures. *Prog. Polym. Sci.*, 29, 1079-1141.

- [50] Liu, J., Rinzler, A. G., Dai, H., Hafner, J. H., Bradley, R. K., Boul, P. J., Lu, A., Iverson, T., Shelimov, K., Huffman, C. B., Rodriguez-Macias, F., Shon, Y. S., Lee, T. R., Colbert, D. T., & Smalley, R. E. (1998). Fullerene Pipes. *Science*, 280, 1253-1256.
- [51] Hirsch, A. (2002). Functionalization of Single-Walled Carbon Nanotubes. *Angew. Chem. Int. Ed.*, 41, 1853-1859.
- [52] Bellayer, S., Gilman, J. W., Eidelman, N., Bourbigot, S., Flambard, X., Fox, D. M., De Long, H. C., & Trulove, P. C. (2005). Preparation of Homogeneously Dispersed Multiwalled Carbon Nanotube/Polystyrene Nanocomposites via Melt Extrusion Using Trialkyl Imidazolium Compatibilizer. *Adv. Funct. Mater.*, 15, 910-916.
- [53] Pötschke, P., Fornes, T. D., & Paul, D. R. (2002). Rheological Behavior of Multiwalled Carbon Nanotube/Polycarbonate Composites. *Polymer*, 43, 3247-3255.
- [54] Liu, L., Qin, Y., Guo, Z. X., & Zhu, D. (2003). Reduction of Solubilized Multi-walled Carbon Nanotubes. *Carbon*, 41, 331-335.
- [55] Wu, T. M., & Chen, E. C. (2006). Crystallization Behavior of Poly(-caprolactone)/Multiwalled Carbon Nanotube Composites. *J. Polym. Sci. Part B: Polym. Phys.*, 44, 598-606.
- [56] Kazarian, S. G., Brantley, N. H., & Eckert, C. A. (1999). Applications of Vibrational Spectroscopy to Characterize Poly(ethylene terephthalate) Processed with Supercritical CO<sub>2</sub>. *Vibrational Spectrosc.*, 19, 277-283.
- [57] Wu, C. S., & Liao, H. T. (2007). Study on the Preparation and Characterization of Biodegradable Polylactide/Multi-walled Carbon Nanotubes Nanocomposites. *Polymer*, 48, 4449-4458.
- [58] Shaffer, M. S. P., & Windle, A. H. (1999). Fabrication and Characterization of Carbon Nanotube/Poly(vinyl alcohol) Composites. *Adv. Mater.*, 11, 937-941.
- [59] Park, S. J., & Cho, M. S. (2000). Thermal Stability of Carbon-MoS<sub>2</sub>-Carbon Composites by Thermogravimetric Analysis. *J. Mater. Sci.*, 35, 3525-3527.
- [60] Abdalla, M., Derrick, D., Adibempe, D., Nyairo, E., Robinson, P., & Thompson, G. (2007). The Effect of Interfacial Chemistry on Molecular Mobility and Morphology of Multiwalled Carbon Nanotubes Epoxy Nanocomposite. *Polymer*, 48, 5662-5670.
- [61] Krishnamoorti, R., Vaia, R. A., & Giannelis, E. P. (1996). Structure and Dynamics of Polymer-Layered Silicate Nanocomposites. *Chem. Mater.*, 8, 1728-1734.
- [62] Abdel-Goad, M., & Pötschke, P. (2005). Rheological Characterization of Melt Processed Polycarbonate-Multiwalled Carbon Nanotube Composites. *J. Non-Newtonian Fluid Mech.*, 128, 2-6.
- [63] Rosedalev, J. H., & Bates, F. S. (1990). Rheology of Ordered and Disordered Symmetric Poly(ethylenepropylene)-poly(ethyl ethylene) Diblock Copolymer. *Macromolecules*, 23, 2329-2338.

- [64] Larson, R. G., Winey, K. I., Patel, S. S., Watanabe, H., & Bruinsma, R. (1993). The Rheology of Layered Liquids: Lamellar Block Copolymers and Smectic Liquid Crystals. *Rheol. Acta*, 32, 245-253.
- [65] Krishnamoorti, R., & Giannelis, E. P. (1997). Rheology of End-tethered Polymer layered silicate Nanocomposites. *Macromolecules*, 30, 4097-4102.
- [66] Pötschke, P., Abdel-Goad, M., Alig, I., Dudkin, S., & Lellinger, D. (2004). Rheological and Dielectrical Characterization of Melt Mixed Polycarbonate-Multiwalled Carbon Nanotube Composites. *Polymer*, 45, 8863-8870.
- [67] Cho, J., & Daniel, I. M. (2008). Reinforcement of Carbon/Epoxy Composites with Multi-wall Carbon Nanotubes and Dispersion Enhancing Block Copolymers. *Scripta Mater.*, 58, 533-536.
- [68] Thostenson, E. T., & Chou, T. W. (2002). Aligned Multi-walled Carbon Nanotube-Reinforced Composites: Processing and Mechanical Characterization. *J. Phys. D: Appl. Phys.*, 35, L77-L80.
- [69] Meng, H., Sui, G. X., Fang, P. F., & Yang, R. (2008). Effects of Acid- and Diamine-modified MWNTs on the Mechanical Properties and Crystallization Behavior of Polyamide 6. *Polymer*, 49, 610-620.
- [70] Cheng, S. Z. D., & Wunderlich, B. (1998). Glass Transition and Melting Behavior of Poly(ethylene 2,6-naphthalenedicarboxylate). *Macromolecules*, 21, 789-797.
- [71] Lopez, L.C., & Wilkes, G.L. (1989). Non-isothermal Crystallization Kinetics of Poly(p-phenylene sulphide). *Polymer*, 30, 882-887.
- [72] Wang, B., Sun, G., Liu, J., He, X., & Li, J. (2006). Crystallization Behavior of Carbon Nanotubes-filled Polyamide 1010. *J. Appl. Polym. Sci.*, 100, 3794-3800.
- [73] Kong, X., Yang, X., Li, G., Zhao, X., Zhou, E., & Ma, D. (2001). Non-isothermal Crystallization Kinetics: Poly(ethylene terephthalate)-Poly(ethylene oxide) Segmented Copolymer and Poly(ethylene oxide). *Homopolymer. Eur. Polym. J.*, 37, 1855-1862.
- [74] Khanna, Y.P. (1990). A Barometer of Crystallization Rates of Polymeric Materials. *Polym. Eng. Sci.*, 30, 1615-1619.
- [75] Avrami, M. (1940). Kinetics of Phase Change. II. Transformation-Time Relations for Random Distribution of Nuclei. *J. Chem. Phys.*, 8(212).
- [76] Ozawa, T. (1971). Kinetics of Non-isothermal Crystallization. *Polymer*, 12, 150-158.
- [77] Jeziorny, A. (1978). Parameters Characterizing the Kinetics of the Non-isothermal Crystallization of Poly(ethylene terephthalate) Determined by DSC. *Polymer*, 19, 1142-1144.
- [78] Dobrev, A., & Gutzow, I. J. (1993). Activity of Substrates in the Catalyzed Nucleation of Glass-forming Melts. I. Theory. *J. Non-Cryst. Solids*, 162, 1-12.

- [79] Kissinger, H.E. (1956). The Crystallization Kinetics with Heating Rate. *Differential Thermal Analysis, J. Res. Natl. Stand.*, 57(217).
- [80] Chen, E. C., & Wu, T. M. (2008). Isothermal and Nonisothermal Crystallization Kinetics of Nylon 6/Functionalized Multi-walled Carbon Nanotube Composites. *J. Polym. Sci. Part B: Polym. Phys.*, 46, 158-169.

IntechOpen

